

Optical design of the Oblique-ECE antenna system for JET

C.Sozzi¹, A.Bruschi¹, A.Simonetto¹, E.DeLaLuna², J.Fessey³, V.Riccardo³
and JET-EFDA Contributors

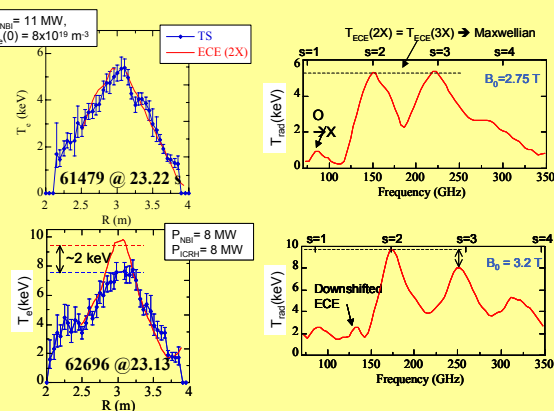
513 ID NUMBER

¹Istituto di Fisica del Plasma, Associazione EURATOM-ENEA-CNR, Milano, Italy

²Asociación EURATOM-CIEMAT, CIEMAT, Madrid, Spain

³EURATOM-UKAEA Association, Culham Science Centre, Abingdon, UK

INTRODUCTION



Systematic disagreements between ECE and Thomson Scattering diagnostics * have substantiated the proposal of the so called Oblique ECE diagnostics on JET, in which the ECE radiation is detected along lines of sight at small angle with respect to the magnetic field gradient, instead of the perpendicular view used in the standard ECE measurements. This layout allows the study of the electron distribution function at low energies revealing any non Maxwellian shape.

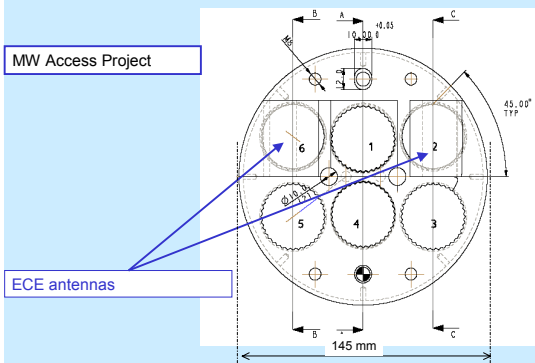
*In particular in the presence of NBI and ICRF heating (TFTR and JET)[1,2], and ECR heating (FTU) [3,4], probably due to deviation of the electron population from Maxwellian-bulk distribution [5].

DESIGN STRATEGY

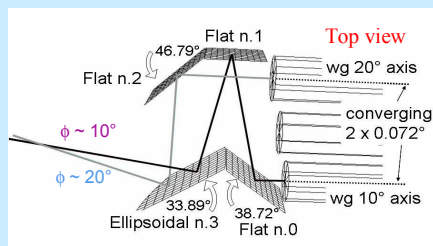
The physics requirements imply two lines of sight at about 10 and 20 degrees respectively in the toroidal direction with respect to the perpendicular to the magnetic field.

The antenna has been designed with three flat mirrors and an ellipsoidal one, the last being shared by the two lines of sight. The mirror arrangement was optimized using electromagnetic calculations performed at several frequencies in the band of the diagnostic, extending from 100 to 400 GHz.

A requirement for any design solution is to avoid interferences between the mirrors and the antenna pattern of the waveguide used for other microwave diagnostics, especially for the adopted configuration with the reflectometry waveguide left in the centre.

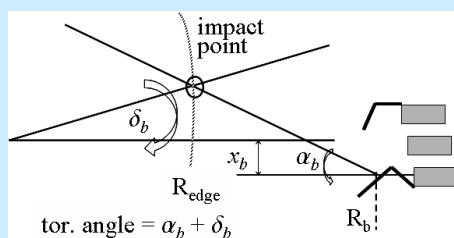


Physical optics model of the ECE oblique antenna. Angles are referred to the central waveguide axis.



The most critical interference for the configuration in figure above occurs at about 90 mm (mirror n.2). This configuration is possible only if a 3*beam (instead of 4) radius clearance is accepted and if this mirror is slightly cut at the bottom together with the top of the lower mirrors in the figure (n. 0 and n. 3). The impact on the ECE oblique pattern at low frequencies has been evaluated with the physical optics calculations presented below.

The more effective solution in focusing the beams at the distance of the plasma edge from the antenna solution was to use only the mirror 3 to focus both the beams, keeping flat all the other mirrors, accepting to have slightly astigmatic beams. The ellipsoid for the last mirror was obtained as a compromise between the optimal ellipsoids for the two beams. As a practical rule, the average incidence angle and the average path length of the central rays emerging from the two waveguide apertures were selected as defining the location of the first focus of the ellipsoidal surface, at 630.67 mm from the mirror centre. The second focus is located at 1550.33mm from the first one, at 10.50° down the axis of the central waveguide. The focal length of the mirror is 441 mm at 180 GHz.



Toroidal angular correction for the antenna main beams.

The input angle at the plasma edge is $\alpha + \delta$ (see figure above) where α is the angle at the antenna output and δ is the angle to the centre of the tokamak of the impact point and is given by the expression:

$$\delta_b = \text{Arc tan} \left[\frac{\text{Tan}(\alpha_b)(R_b - R_{\text{edge}}) - x_b}{R_{\text{edge}}} \right] \quad (1)$$

where the index b denotes the main beam (10° or 20°) and x_b is the offset of the launching point in toroidal direction. Assuming (in mm) $R_{\text{edge}}=3882$, $R_{10^\circ}=4336$, $R_{20^\circ}=4315$, $x_{10^\circ}=35.8$, $x_{20^\circ}=49.1$ we find that $\alpha_{10^\circ}=10.05^\circ$ and $\alpha_{20^\circ}=22.27^\circ$. The figures here used take into account the curvature of the last mirror and the actual path of the central rays of the two beams as calculated by the electromagnetic model. There are severe limitations in the possibility to decrease the actual 20° beam angle: decreasing the mirror 1 inclination would put the beam too close to the mirror 3 edge, causing edge diffraction. On the other hand increasing the mirror 3 inclination would cause mechanical interference with the external supporting structure of the whole antenna system.

ANTENNA PATTERN: PHYSICS OPTICS CALCULATIONS

The antenna model has been verified using the electromagnetic code GRASP8 [6]. The code is able to calculate the electromagnetic scattering from general structures, including successions of plane and curved reflectors. The analysis method used in the case of the Oblique ECE antenna is Physical Optics which is a method to give an approximation to the surface currents valid for perfectly conducting scatterers that are large if compared with the wavelength λ , described by the equation (Collin and Zucker, [7]):

$$\mathbf{J}^e = 2\mathbf{n} \times \mathbf{H}^i \quad (2)$$

Where \mathbf{J}^e is the induced current, \mathbf{n} is the unit surface normal (outward from illuminated surface) and \mathbf{H}^i is the incident magnetic field. The radiated field can then be calculated from

$$\begin{aligned} \mathbf{E} &= -j\omega(\mathbf{A}^e + \frac{1}{k^2}\nabla(\nabla \cdot \mathbf{A}^e)) - \frac{1}{\epsilon}\nabla \times \mathbf{A}^m \\ \mathbf{H} &= \frac{1}{\mu}\nabla \times \mathbf{A}^e - j\omega(\mathbf{A}^m + \frac{1}{k^2}\nabla(\nabla \cdot \mathbf{A}^m)) \end{aligned} \quad (3)$$

Where \mathbf{A} is the vector potential, e and m denote electric and magnetic components, ϵ and μ are electric permittivity and magnetic permeability, ω is the angular frequency and $k=2\pi/\lambda$ is the wavenumber. In the case of the Oblique ECE antenna the illuminating source is the beam propagating from a $\text{TE}_{1,1}$ mode waveguide with aperture diameter of 32 mm. The patterns generated by the two illuminating beams are calculated separately, despite the fact that the ellipsoidal mirror is shared. This procedure has been adopted to avoid undesired interference effects and is justified because the radiation received through the two lobes of the antenna is not coherent.

RESULTS AND CONCLUSIONS

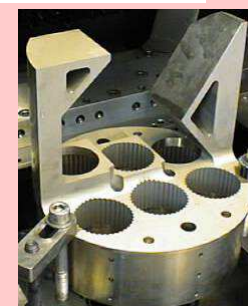
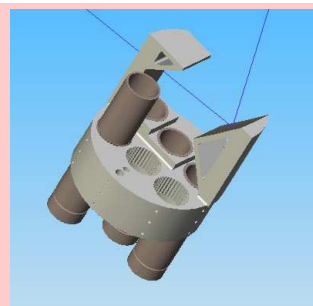
Table below summarizes the results of the GRASP8 simulations. Beam radii (defined as the contours with -8.7 dB, $\approx 1/e^2$, attenuation with respect to the maximum) calculated at 1400 mm from the ellipsoidal mirror of the antenna corresponding to the plasma edge position are reported in the upper side.

The lower side shows an estimation of the angular spread in the toroidal direction, i.e. the maximum longitudinal extension of the -20dB contour around the actual angular direction of each of the main beams of the antenna.

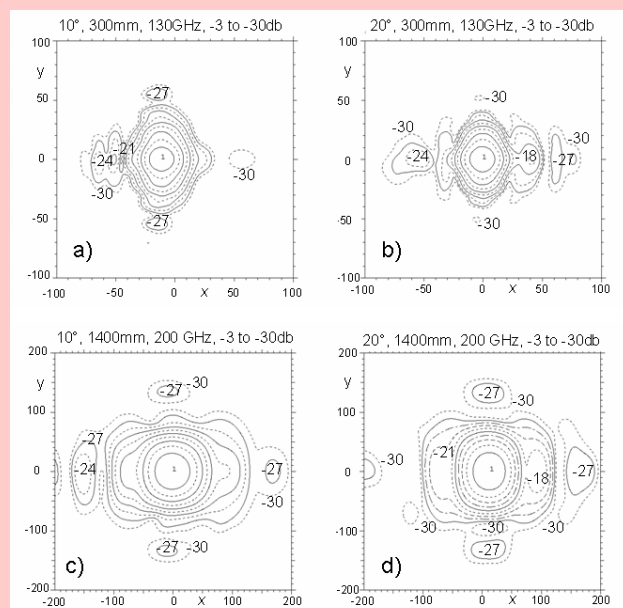
a) equivalent gaussian beam radius (mm)				
beam	100 GHz	130 GHz	200 GHz	400 GHz
20°-x	86.7	66.4	44.7	24.0
20°-y	95.6	76.3	53.0	28.9
10°-x	97.0	74.7	49.8	34.7
10°-y	87.5	72.3	49.8	27.3

b) angular spread (°)				
beam	100 GHz	130 GHz	200 GHz	400 GHz
20° -x	9.1	6.8	4.6	2.5
10° -x	9.5	7.8	4.4	3.1

Performances of the ECE Oblique antenna as evaluated with the simulations above are compliant with the physics requirements of the diagnostics.



ECE oblique antenna, built from a single aluminum piece together with the terminal part of the waveguides. Courtesy Thomas Keating Ltd.



Contour plots of the calculated antenna patterns at 300mm (first row) and at 1400 mm (second row) from the ellipsoidal mirror. In the first row the full scale of the plot is 200x200 mm, in the second row is 400x 400 mm. Each contour line marks a 3dB decrease in the intensity relative to the maximum. Apart from small deformations of the main lobes at level of -18 dB, the secondary lobes are at least 24 dB below the maximum.

ACKNOWLEDGEMENT

This work has been partially supported with the EFDA contract JW4-NEP-ENEA-37.

REFERENCES

- [1] G. Taylor et al., Proc. 9th Joint Workshop on ECE and ECRH, Borrego Spring (1995) p.485
- [2] E. de la Luna et al., Impact of bulk non-Maxwellian electrons on electron temperature measurements, Rev. Sci. Instrum. 74 (2003) p. 1414
- [3] O. Tudisco et al., Electron Cyclotron Heating experiments during the current ramp-up in FTU, 26th EPS Conf. on Contr. Fusion and Plasma Physics, Maastricht (1999), ECA Vol.23J (1999) pp. 101-104
- [4] E. de la Luna, O. Tudisco, et al. Diagnosing the electron distribution function with oblique electron cyclotron emission on FTU. Proceedings of the 12th Joint Workshop on Electron Cyclotron Emission and Electron Cyclotron Heating (ed. by G. Giruzzi, World Scientific, Singapore, 2003), p. 024.
- [5] V. Krivenski, Electron cyclotron emission by non-Maxwellian bulk distribution functions, Fusion Engineering and Design 53 (2001) p. 23
- [6] K.Pontoppidan (Editor), GRASP8 Technical Description, DTK, 2002, Copenhagen pp. 155-164, www.ticra.com
- [7] R.E. Collin and F.J. Zucker, Antenna Theory, Part 1, Chapter 1, McGraw-Hill, 1969, New York